DOI:10.1111/j.1600-0625.2008.00697.x
www.blackwellpublishing.com/EXD

Original Article

Presence of epidermal allantoin further supports oxidative stress in vitiligo

Mohammad Shalbaf[1], Nicholas C. J. Gibbons[1,2], John M. Wood[1], Derek J. Maitland[3], Hartmut Rokos[2], Souna M Elwary[1], Lee K. Marles[1] and Karin U. Schallreuter[1,2]

[1]Clinical and Experimental Dermatology, Department of Biomedical Sciences, University of Bradford, Bradford, UK;
[2]Institute for Pigmentary Disorders in Association with EM Arndt University of Greifswald, Greifswald, Germany and University of Bradford, UK;
[3]Department of Forensic Sciences, School of Life Sciences, University of Bradford, Bradford, UK
Correspondence: Professor Karin U. Schallreuter, Clinical and Experimental Dermatology/Department of Biomedical Sciences, University of Bradford, Bradford, BD7 1DP, West Yorkshire, UK, Tel.: +44 1274 235527, Fax: +44 1274 236849, e-mail: K.Schallreuter@bradford.ac.uk

Accepted for publication 11 January 2008

Abstract: Xanthine dehydrogenase/xanthine oxidase (XDH/XO) catalyses the hydroxylation of hypoxanthine to xanthine and finally to uric acid in purine degradation. These reactions generate H_2O_2 yielding allantoin from uric acid when reactive oxygen species accumulates. The presence of XO in the human epidermis has not been shown so far. As patients with vitiligo accumulate H_2O_2 up to mM levels in their epidermis, it was tempting to examine whether this enzyme and consequently allantoin contribute to the oxidative stress theory in this disease. To address this question, reverse transcription-polymerase chain reaction, immunoreactivity, western blot, enzyme kinetics, computer modelling and high performance liquid chromatography/mass spectrometry analysis were carried out. Our results identified the presence of XDH/XO in epidermal keratinocytes and melanocytes. The enzyme is regulated by H_2O_2 in a concentration-dependent manner, where concentrations of 10^{-6} M upregulates the activity. Moreover, we demonstrate the presence of epidermal allantoin in acute vitiligo, while this metabolite is absent in healthy controls. H_2O_2-mediated oxidation of Trp and Met in XO yields only subtle alterations in the enzyme active site, which is in agreement with the enzyme kinetics in the presence of 10^{-3} M H_2O_2. Systemic XO activities are not affected. Taken together, our results provide evidence that epidermal XO contributes to H_2O_2-mediated oxidative stress in vitiligo via H_2O_2-production and allantoin formation in the epidermal compartment.

Key words: allantoin – human epidermis – hydrogen peroxide – vitiligo – xanthine oxidase

Please cite this paper as: Presence of epidermal allantoin further supports oxidative stress in vitiligo. Experimental Dermatology 2008; 17: 761–770.

Introduction

It has been well documented that the entire epidermis of patients with vitiligo is under oxidative stress because of the accumulation of mM levels of H_2O_2 (1,2). In this context it has been established *in vivo* by fourier-transformed Raman spectroscopy that epidermal H_2O_2 accumulation in patients with vitiligo reaches concentrations in the range of 10^{-3} M (1,3) and these concentrations are sufficient to oxidize Met and Trp residues to Met sulfoxide and to 5-OH-Trp, respectively, in many proteins/enzymes, hormones and peptides (4–8). Several mechanisms in the epidermal compartment have been identified, which generate and degrade H_2O_2 [for review see (9,10)]. Xanthine oxidase (XO, EC 1.1.3.22) produces H_2O_2 in its reaction mechanism and therefore we were interested to test whether this enzyme could be a potential contributor to the H_2O_2 pool in vitiligo.

Xanthine oxidase belongs to the family of the mononuclear molybdopterin co-factor (Moco) containing proteins and is one of the two inter-convertible forms of xanthine oxidoreductase (XOR) containing xanthine dehydrogenase (XDH, EC 1.1.1.204) and in its oxidized form it contains XO. These two enzymes have similar molecular weights and composition of redox centres (11). Under normal physiological conditions, XOR is found in the cell as dehydrogenase. However, under oxidizing conditions, XDH can be immediately converted to the oxidase (12,13). This enzyme exists in different species from bacteria to man (14). In various tissues of mammals, it performs terminal oxidation of all purine bases as the rate-limiting enzyme in the purine degradation pathways (15). XO catalyses the oxidative hydroxylation of hypoxanthine to xanthine followed by xanthine to uric acid conversion accompanied by the generation of H_2O_2 (16) (Scheme 1). Therefore this enzyme is considered as a major biological source for

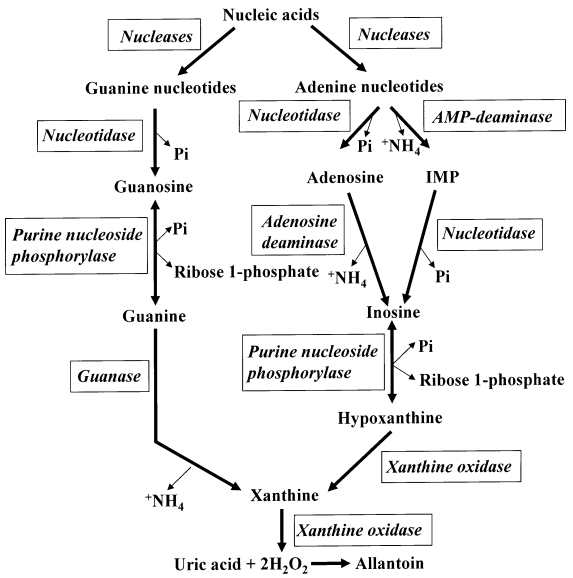

Scheme 1. Purine degradation pathway. Uric acid/allantoin formation from guanine and adenine nucleotides requires xanthine oxidase and produces H_2O_2 (Pi, inorganic orthophosphate; IMP, inosine monophosphate).

generating reactive oxygen species (ROS) in many organs leading to oxidative stress (15,17). Furthermore, this enzyme contains two non-haeme iron atoms in its structure. These can react with H_2O_2 via the Fenton reaction to produce $OH^{\cdot}$; the most potent ROS to initiate DNA damage. However, H_2O_2 oxidizes also uric acid to allantoin. Therefore, this metabolite presents a representative marker for oxidative stress (18–22). Elevated XO levels in plasma of patients with vitiligo have been reported (23).

The aim of this study was first to show the presence and function of XO in epidermal melanocytes (MC) and keratinocytes (KC). The results showed that both cell types transcribe and translate XDH/XO. Moreover, we show that this enzyme is regulated by its own product, H_2O_2, in a concentration-dependent manner. At low concentrations, the enzyme is activated while high concentrations partially inhibit the enzyme besides producing allantoin from uric acid. Given that the structure of XO could potentially be affected by H_2O_2-mediated stress because of oxidation of target amino acids (Met, Trp), as predicted by computer modelling, enzyme kinetics was used to follow the effect of H_2O_2 in the mM range. These results showed that the activity was only partially affected leaving 63% of functioning enzyme, which in turn supported uric acid production followed by allantoin formation. Analysis of epidermal cell extracts from suction blister tissue confirmed the presence of allantoin in patients with acute vitiligo while this product was absent in healthy controls. Analysis of 10 plasma samples of patients with acute vitiligo did not confirm increased XO levels as reported earlier (23). Based on our results, it was concluded that the presence of a functioning XO in the human epidermis can be a major source for H_2O_2 generation leading to allantoin formation in vitiligo.

Materials and methods

Cell cultures

Epidermal MC and KC cultures were established from face thickness human skin (skin phototype III, Fitzpatrick classification; 24) obtained as a surgical waste after cosmetic or non-cosmetic operations as described in detail elsewhere (25,26).

For immuno-reactivity studies, KC or MC were seeded into 8-well chamber slides (Nalge Nunc International, Naperville, IL, USA) and allowed to attach for 48 h followed by rinsing briefly in sterile phosphate-buffered saline (PBS, pH 7.4). Cells were then fixed in ice-cold methanol for 5 min at −20°C and kept at −20°C until further use.

Epidermal mRNA expression of XDH using RT-PCR

Total RNA was extracted from cells before the fourth passage using the Ambion total RNA isolation kit (AMS Biotechnology, Oxon, UK) based on the guanidium isothiocyanate method. cDNA was synthesized using the reverse transcription system (Promega, Southampton, UK) following the manufacturer's protocol. For the PCR amplification of XDH we used the primers reported by Xu 1996 (27). All the primers were obtained from Genosys Biotechnologies Ltd (Pampisford, UK). The sequences for forward and reverse primers were 5′-CTCCGCACAGATATTGTCATGGAT-3′ and 5′-AAATGCCGGGATCTTGTAGGTGCT-3′, respectively. Touch-down PCR was used with the amplification conditions described below; 5 min denaturing at 95°C, followed by 35 cycles for 1 min at 95°C, 1 min at 59.4°C and 1 min at 67°C (decrease of 0.5°C each cycle). Once the PCR cycles were completed, the resulting cDNA strands were separated in 1.2% agarose gel containing ethidium bromide for 90 min. Bands were visualized using the Uvitec camera (Uvitec, Cambridge, UK).

Human skin biopsies

Punch biopsies of 3 mm from normal skin were obtained under local anaesthesia from consented volunteers ($n = 5$; skin phototype III, Fitzpatrick classification) (24). The tissue was embedded in optimal cutting temperature (Sakura, RA Lamb, Eastbourne, UK) at −80°C. After the skin was frozen, 4–5 μm thick cryosections were cut using a Leica CM3050 S cryostat (Leica Microsystems Ltd, Milton Keynes, Buckinghamshire, UK) and placed onto slides coated with poly-L-Lysine (Sigma, Dorset, UK) and stored at −80°C until further use. The study was approved by the

local Ethics Committees and was in agreement with the Declaration of Helsinki Principles.

Cell extracts from epidermal suction blister tissue

Epidermal suction blister tissue was obtained from patient's lesional and non-lesional skin ($n = 10$, mean age = 43.5 years) and healthy age-matched controls ($n = 5$) after written consent using the method of Kiistala (28). All probands had skin phototype III, Fitzpatrick classification. This study was approved by the local Ethics Committees and was in agreement with the declaration of Helsinki.

In situ immunofluorescence studies

To study the immunoreactivity of XDH/XO, slides containing frozen sections were defrosted at room temperature and fixed in ice-cold methanol for 10 min at −20°C and rehydrated in PBS for 5 min. Sections were then blocked in 10% normal donkey serum (NDS) blocking solution in 1% PBS for 90 min at room temperature. This step was followed by incubation with the first primary antibody (1:10 dilution of mouse monoclonal to XO in 1% NDS, Abcam, Cambridge, UK, ab17833) overnight at 4°C. After washing twice in PBS for 5 min, with an intermediate wash in PBS/Tween-20 (0.05%) (Life Science Group; Bio-Rad Laboratories Ltd., Santa Cruz, CA, USA), sections were incubated with a fluorescein isothiocyanate-conjugated donkey anti-mouse secondary antibody (Jackson Immunoresearch Laboratories Inc, PA, USA) at a dilution of 1:100 with 1% NDS for 1 h at room temperature. To study the possible co-localization of XO in MC via double-staining, slides were washed as described above and were blocked in 10% NDS blocking solution in 1% PBS for 90 min at room temperature followed by incubation with a tyrosinase antibody (goat polyclonal, Santa Cruz Biotechnology, Inc., Santa Cruz, CA, USA) overnight at 4°C in the dilution of 1:20. The rest of the procedure was as described above. The secondary antibody in this case was a Tetra methyl Rhodamine Iso-Thiocyanate (TRITC)-conjugated donkey anti-mouse secondary antibody (Jackson Immunoresearch Laboratories) used at a dilution of 1:100 with 1% NDS and incubation for 1 h at room temperature. Slides were washed as above and were dried and mounted in Vectashield Mounting Medium with 4,6-diamino-2-phenylindole (DAPI; Vector Laboratories, Burlingame, CA, USA). Finally sections were viewed with a Leica DMIRB/E fluorescence microscope (Leica Microsystems Ltd, Milton Keynes, Buckinghamshire, UK) and photodocumented using a computer-assisted 3-CCD colour video camera and the IMAGE GRABBER PCI graphics program (both from Optivision, Osset, West Yorkshire, UK). In addition, pictures were captured using a Nikon Eclipse 80i microscope with a DS-U101 Nikon camera (NikonUK Limited, Kingston upon Thames, Survey, UK) coupled to a Nikon ACT-2U capture program (Nikon, (Jasc Software, Inc., Eden Prairie, Minnesota, USA). PAINT SHOP PRO^{TM} 9 was used to merge the two different fluorochromes to follow possible co-localization.

In vitro immunofluorescence labelling of KC and MC

For staining of cultured epidermal cells the same procedure was used as described above. Both KC and MC were again incubated overnight with anti-XDH/XO antibody at the dilution of 1:20 at 4°C. To follow possible expression in melanosomes, MC were incubated with tyrosinase antibody (goat polyclonal, Santa Cruz, CA, USA) overnight at 4°C in the dilution of 1:20.

Quantification of fluorescence intensity

For quantification of XO fluorescence intensity, IPLAB v3.6.5a (Nikon) software was used. The fluorescence was expressed in arbitrary units.

Preparation of melanocyte and keratinocyte cell extracts

Medium was aspirated from the flask and washed with PBS. The attached cells were incubated with trypsin (600 μl per each T-75 flask) for 10 min at 37°C. Cells were gently detached and then were mixed with related media for each type of cell containing trypsin inhibitor. The solution was then centrifuged at 1000 g for 10 min. After removal of the supernatant, the pellet was resuspended in reaction buffer (KH_2PO_4, 0.05 M, pH 7.5) and homogenized on ice. The homogenate was then centrifuged for 1 h at 13 000 g and the supernatant obtained was aliquoted and stored at −80°C until further use.

Preparation of epidermal suction blister cell extracts

The deep frozen tissue was ground with sand in a mortar and taken up in Tris-buffer (0.05 M, pH7.5) as described in detail elsewhere (6). This method allows a very gentle extraction without the danger of any protein denaturation. Samples were aliquoted and stored at −80°C.

Protein determination

Total protein concentrations of cell extracts were determined spectrophotometrically at 280 nm with a Beckman DU-64 UV spectrophotometer (Beckman Coutter Ltd, High Wycombe, Buckinghamshire, UK) as described by Kalb and Bernlohr (29).

Western blot analysis for XDH/XO

Extracts from KC and MC were separated in 10% sodium dodecyl sulfate–polyacrylamide gel electrophoresis and

proteins were transferred to a polyvinylidene difluoride membrane (ImmobilonTM-P; Millipore, Bedford, UK). The membrane was blocked with 3% bovine serum albumin (BSA, Sigma) in tris-buffered saline containing 0.1% (v/v) Tween-20 buffer (TBS-T; 150 mM NaCl, 20 mMTris, 0.047% Tween, pH 7.4) overnight and then incubated with a rabbit biotinylated polyclonal antibody against labelled XO (Abcam, ab20581, dilution 1:10 000) for 3 h. The blot was washed and incubated for 1 h at room temperature with an anti-rabbit horse-radish peroxidase-conjugated antibiotin secondary antibody (Cell Signalling Technology Inc, Danvers, MA, USA) 1:5000, diluted in 1% BSA in TBS-T. Visualization of XDH/XO bands was performed using a modified enhanced chemiluminescence fixed on a film sheet (Sigma, Dorset, UK).

Enzyme purification

To purify bovine milk XO, Pharmacia S-200 column (Pharmacia, Uppsala, Sweden) was used. The column was washed extensively and then equilibrated with buffer containing 0.1 M pyrophosphate (Sigma) and 0.3 mM EDTA (Sigma) pH 8.5 (30). XO (60 mg) (Sigma) was dissolved in 800 μl dH_2O and separated overnight in 1.5 ml fractions. The absorbance was measured at OD_{276} and OD_{450} and the ratio of A_{276} over A_{450} was calculated. Enzyme with a ratio <6.0 was considered pure (30). Two hundered microlitres of aliquots in Eppendorf tubes was kept at −80°C until required.

Enzyme assay

The activity of XO was determined by measuring the rate of oxidation of xanthine to uric acid spectrophotometrically at 290 nm under different conditions. As XO activity generates H_2O_2, the assay was run in the presence and absence of catalase. Standard assays were performed at 25 ± 0.2°C in 0.05 M potassium phosphate buffer (KH_2PO_4, pH = 7.5) containing 100 μM and 0.01 mg/ml final concentration of xanthine (Sigma) and purified XO, respectively. The total volume of the reaction mixture in all experiments was 1 ml. To remove H_2O_2, 0.025 mg/ml of catalase (Sigma) was added to the reaction mixture. This experiment was repeated using varying concentrations of substrate (xanthine, 25, 50, 100 and 200 μM) and H_2O_2 (1, 2.5, 5, 10 and 20 mM; (Fluka, Sigma). To test the activity of XO under severe oxidative conditions, purified XO (25 μg enzyme in each reaction mixture) was incubated with different concentrations of H_2O_2 (0, 5, 10, 20 and 30×10^{-3} M) at room temperature for 2 h. Residual H_2O_2 was removed with Zeba^{TM} Desalt Spin chromatography column (Pierce Biotechnology Inc., Rockford, IL, USA). Catalase was added to all the reaction mixtures. As negative control, a mixture of 200 μl of purified XO (50 μl = 25 μg) with buffer was incubated at room temperature. To confirm the presence of increased XO in plasma/serum of patients with vitiligo as described earlier, we used the same spectrophotometrical test (n = 10 patients, n = 5 controls).

Determination of XO activity of epidermal KC and MC cell extracts using TLC

Xanthine Oxidase activity of epidermal KC and MC cell extracts was determined via a modified thin layer chromatography (TLC) method using [^{14}C]-xanthine (47.5 μCi, Sigma) where the production of [^{14}C]-uric acid by the activity of XO was measured. TLC was performed using either purified XO (for the standard assay) or cell extract prepared from epidermal MC or KC. Because of the UV absorption of uric acid, allantoin and xanthine (all obtained from Sigma), a saturated solution (5 mg/ml) of each was prepared and applied separately for each time point as a series of seven spots onto the 20 × 20 cellulose-coated plates (Fluka, Sigma). Uric acid and allantoin spots were applied on top of the previous series of spots, respectively, followed by visualization under UV (350 nm). For the standard assay, the reaction mixture contained xanthine (0.5 mM cold xanthine and 1 μCi/ml [^{14}C]-xanthine in the final concentration of the reaction mixture), 0.5 mg/ml XO with or without catalase (0.5 mg/ml) all in a final volume of 100 μl KH_2PO_4. For the assay of cell extracts, 50 μl of KC (5 mg/ml) or 90 μl of MC (0.4 mg/ml) cell extract was used instead of XO.

An aliquot of 2 μl was taken after 2, 5, 10, 15, 20, 30 and 40 min and applied onto the previous spots containing saturated xanthine, allantoin and uric acid. The plate was developed at room temperature twice in a solvent (100 ml 1-propanol, 30 ml 8 N ammonium hydroxide and 20 ml dH_2O) up to a distance of 16 cm. R_f values of these compounds were 0.31 ± 0.02, 0.25 ± 0.02 and 0.19 ± 0.04, respectively. After separation the plate was air-dried, the spots were marked under UV, scraped off the plate and transferred into scintillation vials containing 3 ml scintillation liquid (Ready Safe^{TM}, Beckman Coulter Ltd., Fullerton, CA, USA) and counted in [^{14}C] channel (Packard, Tri-Carb 2100TR, Liquid Scintillation Analyser, Packard Instrument Co., Meriden, CT, USA).

Determination of allantoin with HPLC

Allantoin was determined in epidermal suction blister cell extracts using the HPLC method described by George et al. in 2006 (31). These extracts were de-proteinated with perchloric acid ($HClO_4$) on ice for 15 min followed by centrifugation at 13 000 g for 10 min at 4°C. The obtained supernatant was analyzed by HPLC. Analysis was conducted using a Waters 510 pump (Waters Ltd, Elstree Hertfordshire, UK) with a Sphereclone 250 × 4.60 mm C-18 reverse-phase column (Phenomenex, Macclesfield, Cheshire, UK) maintained at 22 °C coupled to a Waters

486 UV detector (Waters Ltd) set at a wavelength of 220 nm. The mobile phase was 10 mM potassium dihydrogen phosphate buffer (KH_2PO_4, pH 4.7) in HPLC grade water (Fisher Chemicals, Loughborough, Leics, UK). The flow rate was maintained at 1.0 ml/min with a pressure of 1900 ± 200 psi. Twenty microlitres of this standard (containing 0.04 μg allantoin in distilled water) was injected. The allantoin peak was identified at a retention time of 3.5 min. Epidermal suction blister cell extracts from acute lesional ($n = 10$), non-lesional ($n = 10$) vitiligo and controls ($n = 5$) were diluted to 1:10 (in mobile phase buffer). Twenty microlitres of each extract was analysed and fractions covering the retention time of 3–4 min (where allantoin elutes) were collected for each sample. To confirm the presence of allantoin, an aliquot of 200 μl of each collected fraction was reanalysed in the presence of 0.04 μg allantoin. Between each run, the column was washed for 30 min. All experiments were carried out in duplicates. Allantoin was confirmed by mass spectroscopy (Quattro Ultima mass spectrometer Waters).

Molecular structural computer modelling of native and oxidized XO

Structural studies of the native and H_2O_2-oxidized Met and Trp residues in the flavin adenine nucleotide (FAD) binding domain, Moco binding domain and the active site of XO were constructed using HYPERCHEM™ software (Gainsville, FL, USA). Deep-view analysis (Institute for Bioinformatics, Lausanne, Switzerland) was used to model the secondary structure minimized in water.

Statistical analysis

The comparison of allantoin levels in epidermal suction blisters was performed using GRAPHPAD PRISM 4 software by the non-parametric Kruskal–Wallis test (one-way ANOVA test). Differences were considered to be significant when $P < 0.05$.

Results

Epidermal mRNA of XDH is expressed in human MC and KC

The capacity for mRNA expression of XDH was tested in human epidermal MC ($n = 2$) and undifferentiated KC ($n = 1$). mRNA expression was demonstrated as a strong band at 177 bp corresponding to the presence of the XDH gene (Fig. 1A).

Presence of XDH/XO in epidermal MC and KC was confirmed by western blot analysis

To substantiate the presence of XDH protein in epidermal cells, western blot analysis was employed. The protein was detected in cytosolic cell extracts from MC and KC. Bands at 145 kDa molecular weight marker corresponded to the monomer of XDH (Fig. 1B).

Immunoreactivity confirms XDH/XO expression *in situ* and *in vitro*

To the best of our knowledge, protein expression of XDH/XO in the human epidermis has never been shown so far. Here, we demonstrate the presence of XDH/XO within the epidermal compartment using immunoreactivity. The protein is present throughout the human epidermis (Fig. 1C). To test whether this protein is also present within MC, we used a melanocyte-specific antibody (anti-tyrosinase) and followed the overlay of both enzymes *in situ* and *in vitro*. Figure 1C (b) shows *in situ* protein expression of tyrosinase in MC which co-localizes with XDH/XO [Fig. 1C (c)]. The enzyme is also expressed *in vitro* in MC and KC [Fig. 1D (b) and E (b)]. Co-localization with tyrosinase indicates the presence of the enzyme within melanosomes [Fig. 1D (d and e)]. Interestingly, XDH/XO seems to be present in the nucleus of both cells [Fig. 1D (f) and E (c)]. The possible role of XO in the nucleus is under further investigation in our laboratory.

XO activities are significantly higher in epidermal KC compared with MC

Xanthine Oxidase activity was determined in cell extracts from epidermal MC and KC by following uric acid formation in the absence of catalase. Maximum [^{14}C] uric acid production was reached at 2 min. The results showed that KC has a significantly higher activity compared with MC (Fig. 2).

XO is activated by H_2O_2 in a concentration-dependent manner

As previously mentioned, XO catalyses the last two steps of the purine degradation pathway leading to uric acid production. H_2O_2 is formed as a product in these oxidation reactions (Scheme 1; 16). To study the activity of the enzyme, the production of uric acid was first followed over 20 min in the presence and absence of catalase using a UV/visible spectrophotometer (Pharmacia Biotech, Ultrospec 2000, Amersham, Buckinghamshire, UK) at 290 nm. The results demonstrated that the addition of catalase reduced the reaction velocity, suggesting that low concentrations of H_2O_2 formed during the reaction increase XO activity (Fig. 3A).

To explore this observation in more detail, we studied the influence of μM H_2O_2 levels on the reaction catalysed by XO following the production of uric acid spectrophotometrically in the presence of saturating substrate (xanthine) and μM levels of H_2O_2. The result proved the activation of the enzyme by low H_2O_2 concentrations (0–200 μM) with an optimum at 70 μM (Fig. 3B).

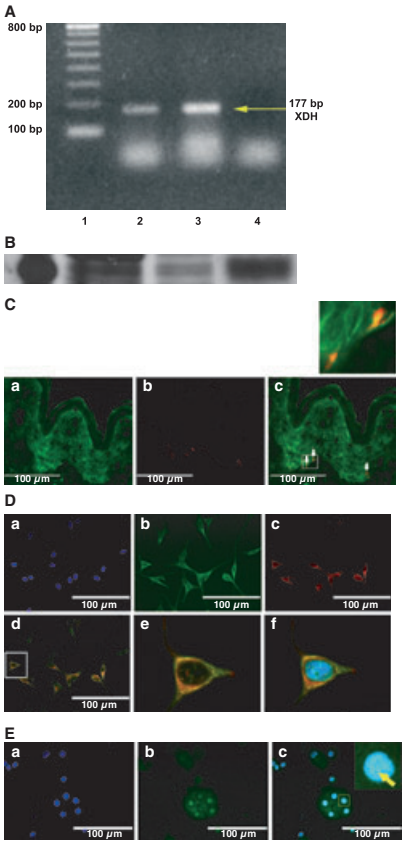

Figure 1. *In situ* and *in vitro* expression of xanthine dehydrogenase/xanthine oxidase (XDH/XO) in the human epidermis. (A) XDH mRNA expression in the human epidermis. PCR amplification of epidermal RNA gave rise to a specific 177 bp product confirming the expression of XDH transcript in both epidermal melanocytes (MC) and keratinocytes (KC). Lane 1 = base pair ladder, Lane 2 = epidermal MC, Lane 3 = epidermal KC, Lane 4 = control. (B) Western blot analysis. (1) Ladder (145 kDa), (2) presence of XO in human epidermal undifferentiated KC (55.2 μg protein loaded), (3) presence of XO in human epidermal MC (55.2 μg protein loaded), (4) XO positive control (0.48 μg purified XO loaded). (C) *In situ* epidermal expression of XDH/XO enzyme (skin phototype III, Fitzpatrick classification). a) *In situ* expression of XDH/XO (labelled fluorescein isothiocyanate-conjugated). b) *In situ* identification of MC (tyrosinase, TRITC-labelled). c) Overlay of a and b identifies co-expression of XO/XDH and tyrosinase in yellow (n = 5). (D). *In vitro expression of XDH/XO in epidermal MC.* a) 4,6-diamino-2-phenylindole (DAPI). b) XDH/XO. c) Tyrosinase. d) Overlay of b and c. e) Close up of two MC suggest the presence of XDH/XO in melanosomes. (E) *XDH/XO expression in KC.* a) DAPI. b) XDH/XO. c) Overlay of a and b suggests the presence of XDH/XO in vesicles and in the nucleus (inset).

H_2O_2 concentrations in the mM range decrease enzyme activity only 37%

To find out more about the direct effect of H_2O_2 on the enzyme, we used purified XO and incubated it with H_2O_2 ($0–30 \times 10^{-3}$ M) for 2 h at room temperature. The reaction was stopped upon addition of 10 μl catalase (10 mg/ml). To ensure that no H_2O_2 was present in the reaction mixture, we used the Zeba™ Desalt Spin chromatography column. Thereafter the activity of the enzyme was assessed. The results revealed that XO is rather stable to H_2O_2-mediated oxidative stress. Even after incubation with 30 mM H_2O_2 over 2 h, the enzyme still showed approximately 63% activity (Fig. 3C). A more detailed analysis showed decreased uric acid formation besides inhibition of the enzyme (Fig. 3D). These results suggested oxidation/degradation of uric acid to allantoin.

H_2O_2 yields oxidation of uric acid to allantoin

To test the formation of uric acid and its possible oxidation/degradation to allantoin by H_2O_2 over time, we used TLC and [^{14}C]-xanthine in the presence and absence of catalase. The result showed that uric acid formation is time-dependent and in the absence of catalase. In the presence of catalase, uric acid formation increased constantly, whereas in the absence of catalase after an initial increase, uric acid was indeed oxidized to allantoin by H_2O_2 produced during the reaction [Fig. 4A (a and b)].

Allantoin is present in the epidermis of acute vitiligo

As allantoin is a marker for H_2O_2-mediated oxidation of uric acid, and epidermal H_2O_2 concentrations in patients with vitiligo exceeded mM concentrations of this ROS, we decided to test the formation of allantoin in epidermal cell extracts from suction blister tissue originating from active vitiligo (n = 10). Allantoin was determined via HPLC and the correct assignment was confirmed by mass spectrometry (data not shown). The results of this study confirmed that allantoin is indeed present in both lesional and non-lesional epidermis of acute vitiligo (n = 10), whereas healthy controls (n = 5) do not show this metabolite (Fig. 4B).

As documented earlier that using a spectrophotometric assay, plasma/serum XO levels increased in patients with vitiligo (23) and based on our results presented above, it was decided to evaluate serum XO levels in 10 patients with acute vitiligo and in five healthy controls using the same methodology. Our results did not confirm the increase of systemic XO activities (data not shown) as reported by Koca et al. (23). Taking into consideration that our enzyme kinetics showed that only pure XO can be used for the spectrophotometric assay while a much more sensitive isotope assay was needed to evaluate XO activities in cell extracts, this result is not surprising.

Computer simulation suggests minor structural alteration by H_2O_2-mediated oxidation for XO explaining the subtle effect on enzyme activity

Finally, to obtain a better understanding on the effects of H_2O_2 on XO activity, we utilized computer simulation

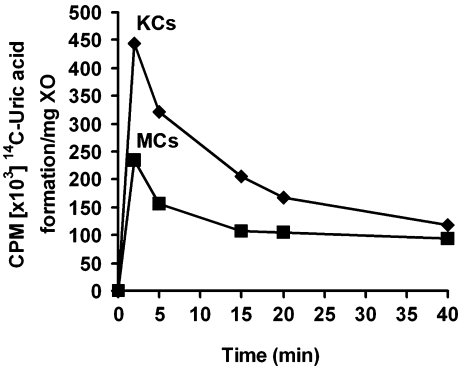

Figure 2. [^{14}C]-uric acid formation in human epidermal melanocytes (MC) and keratinocytes (KC) cell extracts. The result indicates that both epidermal cells have xanthine oxidase activity but KC have double the activity compared with MC.

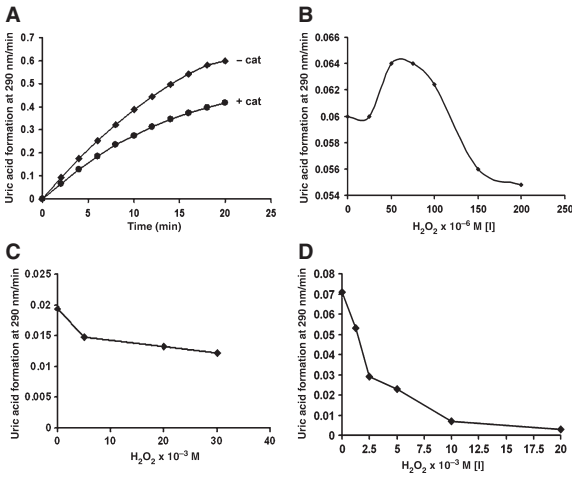

Figure 3. The influence of H_2O_2 on xanthine oxidase (XO) activity. (A) Uric acid formation from the oxidation of xanthine by XO at 290 nm both in the absence and presence of catalase. The graph shows that catalase slows down the production of uric acid indicating that low concentrations of H_2O_2 produced during the reaction yield an increase in enzyme activity. (B) (V)Au: Please define: [V]. versus inhibitor (I) analysis. Activation of XO by μM range (0–200) of H_2O_2 concentrations shows an increase in enzyme activity. (C) The activity of XO after preincubation over 2 h with different H_2O_2 concentrations at room temperature. The graph shows that the oxidized enzyme (5 mM H_2O_2) is still around 75% active. (D) (V) versus inhibitor (I) analysis suggesting both inhibition of the enzyme or decrease in product formation because of further oxidation of the product by mM concentrations of H_2O_2.

employing HYPERCHEM^{TM} software and a deep-view analysis to ascertain structural changes for XO before and after oxidation of Met and Trp residues in the structure with H_2O_2. As mentioned earlier, XO has three main domains: (i) reduced flavin adenine nucleotide ($FADH_2$) binding domain, (ii) the binding domain for the co-factor Moco and (iii) an active site binding domain. The effect of H_2O_2-mediated oxidation was investigated in all three domains.

$FADH_2$-binding

Computer simulation suggests oxidation of Trp and Met residues around the $FADH_2$ binding domain by H_2O_2 causes minor changes affecting π-π stacking and H-bonding network around that domain. However, this disruption is not enough to significantly affect the affinity of XO for FAD and it may only affect the vulnerability of $FADH_2$ to oxidation (Fig. 5A and B).

Co-factor binding is not altered

Oxidation of Trp and Met residues around the Moco-binding domain does not affect binding (Fig. 5C and D).

H_2O_2 affects the active site of XO

Oxidation of Trp and Met residues around the active site causes shifts in the positions of several residues. Six residues are involved in the active site of XO. Among them, Glu^{1261} is the crucial catalytic residue in the active site of XO and Arg^{880}, Phe^{914} and Phe^{1009} are involved in forming a binding site for the substrates or inhibitors. Therefore shifting the position of these amino acids via oxidation by H_2O_2 seems to affect the reaction rate and catalysis of the XO (Fig. 5E and F). The latter result is in agreement with the reduction of enzyme activity of the oxidized XO towards uric acid production as the oxidized enzyme (after incubation with 30 mM H_2O_2 for 2 h) loses 37% of its activity (Fig. 3C).

Discussion

It has been well documented that the entire epidermis of patients with vitiligo is under oxidative stress because of accumulation of mM range of H_2O_2 (1,10,32). Moreover, it has been also shown that these patients suffer from systemic oxidative stress (5,23,33,34). As XO plays a major biological role in generating oxygen-derived ROS (H_2O_2, $OH^{\bullet}$) in many organs (15), the presence and activity of this enzyme in epidermal cells was of interest in general and especially in the context of vitiligo. To the best of our knowledge, we here demonstrate for the first time that mRNA and protein expression and enzyme activities of this enzyme are present in both epidermal MC and KC. In MC, XO is predominantly distributed around the nucleus in a granular pattern, where it co-localizes with tyrosinase suggesting that XO could be present in melanosomes. Our results also show that XO is present in undifferentiated KC. Moreover, co-localization with DAPI suggests the presence of XO in the nucleus of both cell types. This observation needs further investigation. Enzyme activities are higher in KC compared with MC.

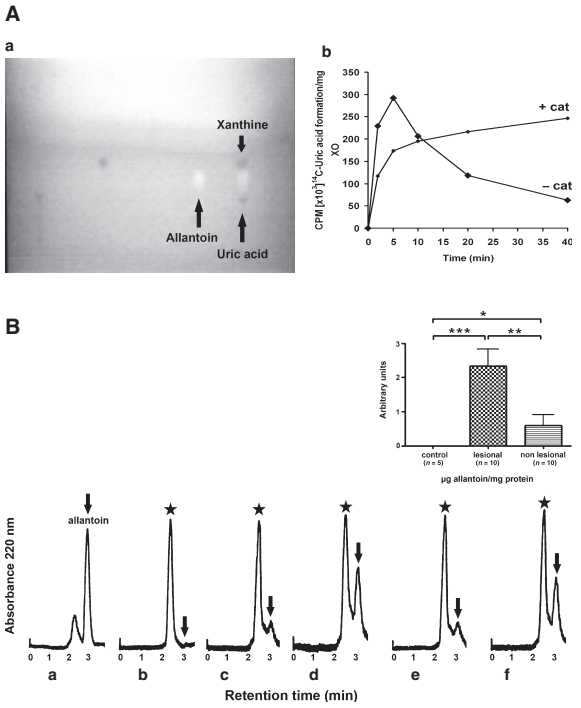

Figure 4. (A) Oxidation of uric acid by H_2O_2 yields allantoin. (a) Thin layer chromatography identifies allantoin as an oxidation product of uric acid. (b) [^{14}C] uric acid formation over the time shows that in the absence of catalase (–cat), uric acid formation increases up to 5 min and then decreases, implying oxidation of uric acid to allantoin by H_2O_2 produced during the reaction. This assumption is supported by the increase in uric acid formation in the presence of catalase (+cat). (B) High performance liquid chromatography proves the presence of allantoin in the epidermis of vitiligo. (a) Twenty microlitre allantoin solution (Standard, 0.04 μg allantoin) was injected, and allantoin eluted at a retention time of 3 min. (b) Healthy control extract does not show any allantoin. (c) The presence of allantoin in lesional epidermis of acute vitiligo was detected at 3 min. (d) Sample spiked with allantoin standard confirmed the correct retention time. (e) The presence of allantoin in non-lesional epidermis of acute vitiligo was detected at 3 min. (f) Sample spiked with allantoin standard confirmed the correct retention time. ★ Uncharacterized peak (under investigation), arrows indicate allantoin peak. Inset: Allantoin levels are absent in healthy controls. Levels in lesional skin of patients with vitiligo are significantly higher compared with non-lesional skin ($P < 0.05$). The presence of allantoin in epidermal cell extracts was confirmed by mass spectroscopy (data not shown).

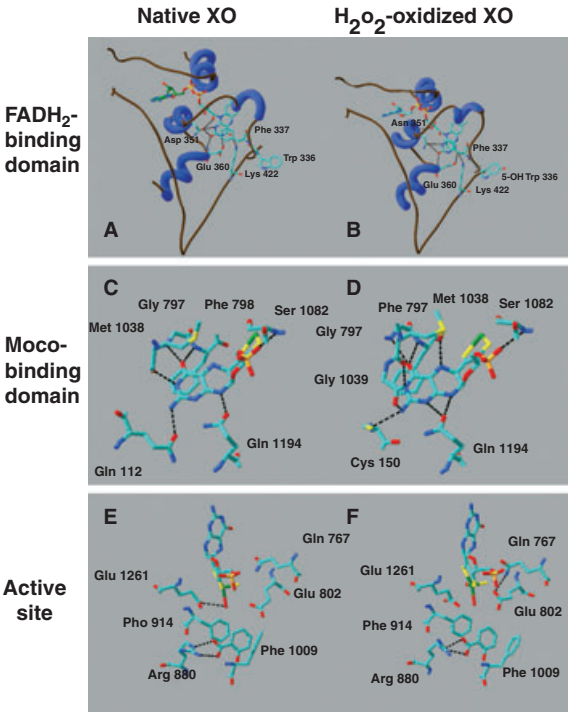

Figure 5. Comparison of computer-simulated native and H_2O_2-oxidized xanthine dehydrogenase/xanthine oxidase (XDH/XO) [$FADH_2$ binding domain, molybdopterin (Moco) binding domain and the active site of XO]. *Native enzyme.* (i) $FADH_2$ binding domain: The flavin ring of $FADH_2$ is bound via H-bonds from Asp^{351}, Glu^{360} and Lys^{422} and via π-π stacking interactions with the phenyl ring of Phe^{337}. (ii) Molybdopterin (Moco) binding domain: Moco is bound by H-bonds from the residues Gln^{112}, Gly^{797}, Phe^{798}, Met^{1038}, Ser^{1082} and Gln^{1194}. (iii) Active site of XDH/XO: Six residues are involved in the active site of XO. Glu^{1261} is the crucial catalytic residue, while Gln^{767} and Glu^{802} are involved in aiding catalysis. Arg^{880}, Phe^{914} and Phe^{1009} are involved in the formation of a binding site for the substrates or inhibitors. Arg^{880} acts to form H-bonds/salt bridges while Phe^{914} and Phe^{1009} are involved in π-π stacking interaction with the aromatic rings of substrates/inhibitors. *Oxidized enzyme.* (i) $FADH_2$ binding domain: Oxidation of Met and Trp residues around the $FADH_2$ binding (most noticeable Trp^{336} shown here) disrupts π-π stacking of Phe^{337} and the H-bonding network to a small extent. While this is not enough to significantly affect the affinity of XO for $FADH_2$, it may affect the vulnerability of $FADH_2$ to oxidation. (ii) Molybdopterin binding domain: Oxidation of Met and Trp residues does not adversely affect binding, with only 1 H-bond being lost from Gln^{112} and several new ones being formed, one additional bond is formed from both Met^{1038} and Gln^{1194} and two completely new H-bonds formed from Cys^{150} and Gly^{1039}. (iii) Active site of XDH/XO: Oxidation of Met and Trp residues around the active site causes shift in the positions of several residues. Phe^{914} and Phe^{1009} do not seem to be affected at all, while Gln^{767}and Glu^{802} appear to be shifted into positions that may enable them to interact more strongly with the Moco-factor. Arg^{880} and Glu^{1261} are shifted away from their positions, affecting reaction rate and catalysis.

H_2O_2 is a product of the XO reaction that is formed during the reaction (Scheme 1) and this ROS is removed under normal conditions by catalase. As XO contains iron in its structure which can react with H_2O_2 via the Fenton reaction to produce the very reactive $OH^{\cdot}$ radicals, we followed the kinetics of the enzyme in the presence and absence of excess H_2O_2. Our results revealed that low concentrations activate the enzyme while higher concentrations decrease enzyme activity 37% (Fig. 3B and C). We were able to show that the observed decreased enzyme reaction was the result of decreased uric acid formation because of oxidation of the product to allantoin by H_2O_2 originating from the reaction (35).

To explore the effect of H_2O_2 on the enzyme structure in detail, we used computer molecular modelling. The analysis revealed that oxidation of Trp around the $FADH_2$ binding site (Trp^{336}) disrupts π-π stacking of Phe^{337} and H-bonding network to a small extent. However, this little change would not significantly affect the affinity of XO for $FADH_2$ but it could affect the vulnerability of $FADH_2$ to oxidation (Fig. 5A and B). Moreover, this analysis also showed that the oxidation of Met and Trp residues does not adversely influence the co-factor binding site (Fig. 5C and D), whereas oxidation of Met and Trp residues around the active site causes shifts in the positions of several amino acid residues, explaining the decreased reaction rate during catalysis (Fig. 5E and F).

As H_2O_2 can oxidize uric acid, consequently the formation of allantoin in humans has been considered as a reliable biomarker for oxidative stress (18–22). Allantoin is a product in purine metabolism in mammals except primates and is normally excreted in urine. This product is formed from the oxidation of uric acid by the enzyme urate oxidase (35). Despite the fact that humans lack this enzyme, allantoin has been measured in urine and plasma (18–20,36). Considering vitiligo as a biological model for epidermal oxidative stress, we postulated the presence of allantoin in the lesional epidermis of acute vitiligo. Our results show indeed the presence of this metabolite in the lesional and non-lesional skin of all patients with acute vitiligo while it is absent in healthy controls (Fig. 4B). In summary, our findings add to the list of oxidative stress in the pathophysiology in vitiligo. The presence of epidermal allantoin in acute vitiligo mirrors and emphasizes the involvement of H_2O_2-mediated oxidative stress in this disease. Future work needs to show whether this metabolite is of any significance in other dermatoses. Importantly, systemic serum XO is not affected by epidermal H_2O_2 in this disease (23).

Conflict of Interest

The authors declare no conflict of interest.

Acknowledgements

This research was supported by Stiefel International with a grant to KUS, the Deutsche Vitiligo-Verein and private donations. The presented results are part of an ongoing PhD thesis (MS).

References

1 Schallreuter K U, Moore J, Wood J M *et al.* In vivo and in vitro evidence for hydrogen peroxide (H_2O_2) accumulation in the epidermis of patients with vitiligo and its successful removal by a UVB-activated pseudocatalase. J Investig Dermatol Symp Proc 1999: **4**: 91–96.

2 Schallreuter K U. A review of recent advances on the regulation of pigmentation in the human epidermis. Cell Mol Biol (Noisy-le-grand) 1999: **45**: 943–949.

3 Wood J M, Chavan B, Hafeez I, Schallreuter K U. Regulation of tyrosinase by tetrahydropteridines – what is real? A critical re-analysis of H. Wojtasek's view. Biochem Biophys Res Commun 2005: **331**: 891–893.

4 Schallreuter K U. Functioning methionine-S-sulfoxide reductases A and B are present in human skin. J Invest Dermatol 2006: **126**: 947–949.

5 Hasse S, Gibbons N C, Rokos H, Marles L K, Schallreuter K U. Perturbed 6-tetrahydrobiopterin recycling via decreased dihydropteridine reductase in vitiligo: more evidence for H_2O_2 stress. J Invest Dermatol 2004: **122**: 307–313.

6 Schallreuter K U, Moore J, Wood J M *et al.* Epidermal H_2O_2 accumulation alters tetrahydrobiopterin ($6BH_4$) recycling in vitiligo: identification of a general mechanism in regulation of all $6BH_4$-dependent processes? J Invest Dermatol 2001: **116**: 167–174.

7 Schallreuter K U, Elwary S M, Gibbons N C, Rokos H, Wood J M. Activation/deactivation of acetylcholinesterase by H_2O_2: more evidence for oxidative stress in vitiligo. Biochem Biophys Res Commun 2004: **315**: 502–508.

8 Wood J M, Schallreuter K U. UVA-irradiated pheomelanin alters the structure of catalase and decreases its activity in human skin. J Invest Dermatol 2006: **126**: 13–14.

9 Schallreuter K U, Rubsam K, Gibbons N C *et al.* Methionine sulfoxide reductases A and B are deactivated by hydrogen peroxide (H_2O_2) in the epidermis of patients with vitiligo. J Invest Dermatol 2007: doi: 10.1038/sj.jid.5701100

10 Schallreuter K. Oxidative stress in human epidermis. G Ital Dermatol Venereol 2005: **140, No. 5**: 505–514.

11 Hille R, Nishino T. Flavoprotein structure and mechanism. 4. Xanthine oxidase and xanthine dehydrogenase. FASEB J 1995: **9**: 995–1003.

12 Glantzounis G K, Tsimoyiannis E C, Kappas A M, Galaris D A. Uric acid and oxidative stress. Curr Pharm Des 2005: **11**: 4145–4151.

13 Enroth C, Eger B T, Okamoto K, Nishino T, Nishino T, Pai E F. Crystal structures of bovine milk xanthine dehydrogenase and xanthine oxidase: structure-based mechanism of conversion. Proc Natl Acad Sci U S A 2000: **97**: 10723–10728.

14 Al-Khalidi U A, Chaglassian T H. The species distribution of xanthine oxidase. Biochem J 1965: **97**: 318–320.

15 Parks D A, Granger D N. Xanthine oxidase: biochemistry, distribution and physiology. Acta Physiol Scand Suppl 1986: **548**: 87–99.

16 Mathews C K, van Holde K E, Ahern K G. Biochemistry. Benjamin/Cummings, an imprint of Addison Wesley Longman, San Francisco, CA, USA, 2000.

17 Nishino T, Okamoto K, Kawaguchi Y *et al.* Mechanism of the conversion of xanthine dehydrogenase to xanthine oxidase: identification of the two cysteine disulfide bonds and crystal structure of a non-convertible rat liver xanthine dehydrogenase mutant. J Biol Chem 2005: **280**: 24888–24894.

18 Benzie I F, Chung W, Tomlinson B. Simultaneous measurement of allantoin and urate in plasma: analytical evaluation and potential clinical application in oxidant:antioxidant balance studies. Clin Chem 1999: **45**: 901–904.

19 Grootveld M, Halliwell B. Measurement of allantoin and uric acid in human body fluids. A potential index of free-radical reactions in vivo? Biochem J 1987: **243**: 803–808.

20 Kaur H, Halliwell B. Action of biologically-relevant oxidizing species upon uric acid. Identification of uric acid oxidation products. Chem Biol Interact 1990: **73**: 235–247.

21 Yardim-Akaydin S, Sepici A, Ozkan Y, Simsek B, Sepici V. Evaluation of allantoin levels as a new marker of oxidative stress in Behcet's disease. Scand J Rheumatol 2006: **35**: 61–64.

22 Yardim-Akaydin S, Sepici A, Ozkan Y, Torun M, Simsek B, Sepici V. Oxidation of uric acid in rheumatoid arthritis: is allantoin a marker of oxidative stress? Free Radic Res 2004: **38**: 623–628.

23 Koca R, Armutcu F, Altinyazar H C, Gurel A. Oxidant-antioxidant enzymes and lipid peroxidation in generalized vitiligo. Clin Exp Dermatol 2004: **29**: 406–409.

24 Fitzpatrick T B, Miyamoto M, Ishikawa K. The evolution of concepts of melanin biology. Arch Dermatol 1967: **96**: 305–323.

25 Spencer J D, Chavan B, Marles L K, Kauser S, Rokos H, Schallreuter K U. A novel mechanism in control of human pigmentation by {beta}-melanocyte-stimulating hormone and 7-tetrahydrobiopterin. J Endocrinol 2005: **187**: 293–302.

26 Spencer J D, Gibbons N C, Rokos H, Peters E M, Wood J M, Schallreuter K U. Oxidative stress via hydrogen peroxide affects Pro-opiomelanocortin peptides directly in the epidermis of patients with vitiligo. J Invest Dermatol 2006: **127**: 411–420.

27 Xu P, Hueckstead T P, Hoidal J R. Molecular cloning and characterization of the human xanthine dehydrogenase gene (XDH). Genomics 1996: **34**: 173–180.

28 Kiistala U. Suction blister device for separation of viable epidermis from dermis. J Invest Dermatol 1968: **50**: 129–137.

29 Kalb V F, Jr. Bernlohr R W. A new spectrophotometric assay for protein in cell extracts. Anal Biochem 1977: **82**: 362–371.

30 Stockert A L. Spectroscopic and kinetic studies of bovine xanthine oxidase and Rhodobacter capsulatus xanthine dehydrogenase (PhD thesis). The Ohio state University, Columbus, Ohio: Department of Medical Biochemistry, 2004.

31 George S K, Dipu M T, Mehra U R, Singh P, Verma A K, Ramgaokar J S. Improved HPLC method for the simultaneous determination of allantoin, uric acid and creatinine in cattle urine. J Chromatogr B Analyt Technol Biomed Life Sci 2006: **832**: 134–137.

32 Schallreuter K U. Successful treatment of oxidative stress in vitiligo. Skin Pharmacol Appl Skin Physiol 1999: **12**: 132–138.

33 Dell'Anna M L, Ottaviani M, Albanesi V *et al.* Membrane lipid alterations as a possible basis for melanocyte degeneration in vitiligo. J Invest Dermatol 2007: **127**: 1226–1233.

34 Maresca V, Roccella M, Roccella F *et al.* Increased sensitivity to peroxidative agents as a possible pathogenic factor of melanocyte damage in vitiligo. J Invest Dermatol 1997: **109**: 310–313.

35 Newsholm E A, Leech A R. Biochemistry for the Medical Sciences. John Wiley & Sons, Inc., Wiley Europe Ltd, Chicheste, UK, 1984.

36 Simoyi M F, Falkenstein E, Van Dyke K, Blemings K P, Klandorf H. Allantoin, the oxidation product of uric acid is present in chicken and turkey plasma. Comp Biochem Physiol B Biochem Mol Biol 2003: **135**: 325–335.